BEST AVAILABLE IMAGES

Defective images within this document are accurate representations of the original documents submitted by the applicant.

Defects in the images may include (but are not limited to):

- BLACK BORDERS
- TEXT CUT OFF AT TOP, BOTTOM OR SIDES
- FADED TEXT
- ILLEGIBLE TEXT
- SKEWED/SLANTED IMAGES
- COLORED PHOTOS
- BLACK OR VERY BLACK AND WHITE DARK PHOTOS
- GRAY SCALE DOCUMENTS

IMAGES ARE BEST AVAILABLE COPY.

As rescanning documents *will not* correct images, please do not report the images to the Image Problem Mailbox.

Configurational and Electrical Behavior of Ni-YSZ Cermet with Novel Microstructure for Solid Oxide Fuel Cell Anodes

P.d.02-1997
P.641-646 = (6)

Hibiki Ito, Tohru Yamamoto, and Masashi Mori

Central Research Institute of Electric Power Industry, 2-6-1 Nagasaka, Yokosuka, Kanagawa 240-01, Japan

Teruhisa Horita, Natsuko Sakai, Harumi Yokokawa,* and Masayuki Dokiya*

National Institute of Materials and Chemical Research, 1-1 Higashi, Tsukuba, Ibaraki 305, Japan

ABSTRACT

A novel Ni-YSZ cermet anode for solid oxide fuel cell application has been developed in order to solve problems with our previous anode, which was prepared from a powder mixture of NiO and precalcined YSZ. In contrast to homogeneously sized YSZ in our previous anode, the new material has a YSZ frame made of coarse (average size of 27.0 μm) and fine (average size of 0.6 μm) powders to sustain the network of Ni and pore. Unlike the previous anode, no significant changes in shrinkage and microstructure of the new anodes were detected during sintering in air and upon transformation of NiO to Ni metal in a reducing atmosphere. The influence of the content of coarse YSZ powder was examined by fixing the Ni volume ratio at 40%. It has been found that with an increasing amount of coarse YSZ powder, the electrical conductivity increased by three orders of magnitude around 20 weight percent (w/o) coarse YSZ powder and also that the anode with an 80 w/o one was found to be the most stable during cell fabrication and cell operation. It is concluded that the consolidated framework made from two distinctly sized particles leads to a more stable YSZ frame and Ni network.

Introduction

Electrodes for fuel cells and batteries provide sites for electrode reactions and electrical paths under generation of electricity. In solid oxide fuel cells (SOFCs), nickel (Ni) and yttria stabilized zirconia (YSZ) cermets are usually used as the anode material. The latter is added to make the thermal expansion coefficient of the anode compatible with the other cell components, especially YSZ electrolyte, and to inhibit the agglomeration of Ni particles.[1] Optimizing the distribution of Ni particles in the anode layer would increase the amount of electrode reaction sites, in other words, the length of three-phase boundary[2] and the formation of current path.[3,4] A network of micropores in the anode is required to provide a diffusion path for gaseous reactants and products. These functions depend strongly on the morphological features of the anode consisting of Ni particles, added YSZ, and micropores.

Studies on anode materials have been focusing on lowering the overpotential and clarifying the anodic reaction mechanism,[5-8] and several attempts have been reported to improve the long-term stability of cermet anodes. Since metal ruthenium (Ru) has a higher melting point than Ni, a Ru-YSZ cermet has been examined by Ippommatsu *et al.*[9,10] Murakami *et al.*[11] have suggested that adding ZrO_2 fiber would improve the anode/electrolyte adherence and decrease the overall shrinkage, leading to improved long-term stability. Iwasawa *et al.*[12] have tried to prevent Ni particle coagulation by preheat-treatment of the cermet powders.

Investigations at CRIEPI have showed that during long-term fuel cell conditions, there occurs a significant drop in cell performance with our previous anode material; specifically, a current density decreased to 0.2 A/cm^2 (even at a short circuit) for about 40 h. It has been already proven that this behavior was not due to a chemical interfacial reaction between cathode and electrolyte.[13,14] Polarization phenomena on this anode were investigated, and the microstructures were observed. Results of these examinations indicated that this performance drop was due to anode degradation which was caused by the agglomeration of Ni particles and the resulting compaction of the anode layer.[15,16] As Dees *et al.* reported,[17] agglomeration of Ni particles under operating conditions leads to a diminishment of reaction sites and cutting off on current paths. Furthermore, the shrinkage of the electrode upon firing also leads to a decrease in the gas permeability of the electrode layer, occurrence of shearing stress at the electrolyte/electrode interfaces, and an increase in the contact resistance between the electrode and a current collector when assembled as a stack.

On the basis of the above examination of the dimensional stability of the anode and its relation to the long-term stability of cell performance, we have proposed a novel anode microstructure to solve the problems mentioned above. The uniqueness of this new anode is that YSZ powders are divided into two kinds, coarse and fine.[15,16] It was found that no changes in the cell voltage were observed under a constant current flow of 0.4 A/cm^2 when this new anode used. Figure 1 shows the anode overpotentials at 0.2 A/cm^2 for the two anodes during a long-term operation. The curve of the previous anode rose abruptly after about 20 h, whereas the new one kept the overpotential constant. These results have revealed that the new anode with the novel microstructure dramatically improves long-term stability.

In this study, further experimental results on these anode materials are reported and discussed in terms of the changes in the configuration and the electrical conductivity under a reduction atmosphere.

Experimental

Sample preparation.—The previous anode as a reference material, with 40 volume percent (v/o) Ni metal in the

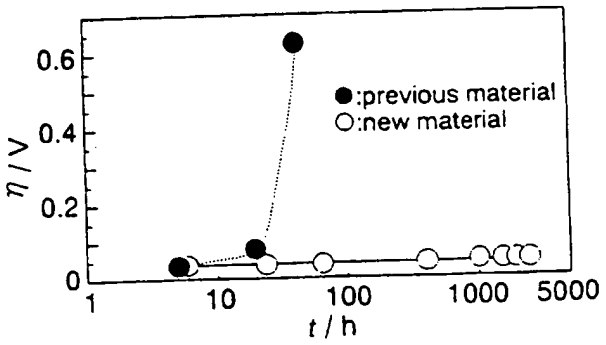

Fig. 1. Changes in anodic overpotential, η, as a function of operating time, *t*, at 0.2 A/cm^2 under cell generation test. These data were obtained with a galvanostatic current interruption technique.

* Electrochemical Society Active Member.

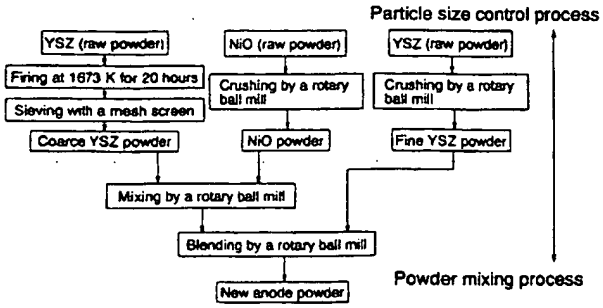

Fig. 2. Preparation process of new anode for the present investigation. This process has two main steps; the first is a particle size control step and the second is a powder mixing step. In the second step, care was exercised not to crush the coarse YSZ particles.

reduced state, was prepared from a powder mixture of nickel oxide (NiO) and precalcined YSZ with homogeneous particle size distribution (average particle size of 5.0 μm). Details of the preparation process have been described elsewhere.[15,16]

The preparation procedure of the new anode material consists of two main steps, as shown in Fig. 2. The first step involves the control of particle size distribution; coarse YSZ (TZ-8Y, TOSOH Corp.) was obtained by heating at 1673 K for 20 h in air and subsequent sieving with a 330 mesh screen. Respective fine YSZ (TZ-8Ys, TOSOH Corp.) and NiO (Nakalai-tesque Inc.) were pulverized with ethanol in a rotary ball mill. In the second step, these powders were mixed, but to prevent the crushing of the coarse YSZ particle, soft balls and a soft vessel were used in a dry process. The Ni metal content of all the anodes was fixed at 40 v/o of the total material, while several different ratios of coarse YSZ to fine YSZ were used to produce new cermet anodes; they are designated as APx (the number, x, means the weight ratio of coarse YSZ to the amount of YSZ, ranging from 0 to 11).

Measurement of anode characteristics.—For reduction test and electrical conductivity measurement, the anode powders were molded at a pressure of around 20 MPa and then sintered at 1673 K for 10 h. The samples were placed in an alumina tube and held in a hydrogen flow of 100 cm^3/min at 1273 K for 12 to 300 h. Oxygen partial pressure in the hydrogen flow is at about 4.49×10^{-16} Pa, measured by an oxygen sensor with YSZ electrolyte.

The reduction test was carried out for a selected period of time. The size and weight of the samples were then measured to derive the volume and porosity. The electrical conductivity measurements were made after the reduction test by ac impedance spectroscopy and/or the dc four-probe method under a H_2 atmosphere at 1273 K. The samples were set in a special rig, similar to that used by MacDonald.[18]

Results and Discussion

Observation of microstructures.—The microstructure of the anode samples was observed and analyzed with an electron probe microanalyzer (EPMA, JEOL Ltd., JXA-8900R). For the reference anode, no changes were detected under secondary electron imaging (SEI) before and after the cell generation test. Under the Ni elemental distribution map after the test, however, it was found that the Ni particles agglomerated at several places causing disconnections in the Ni network.[15] Figure 3 shows typical microstructures of the new anode before and after the reduction test. This is the same material as that used in the long-term operation. The Zr elemental distribution map showed that the fine YSZ particles formed bridges that connected the coarse YSZ particles. Note that the fine but slightly sintered YSZ surrounds Ni particles. This suggests that the fine YSZ is effective in adhering the coarse YSZ particles and fixing the Ni particles. Even after the cell tests for about 3000 h, the firmly connected network of Ni particles still extended from the electrolyte/electrode interface to the opposite side of the anode layer.[15] Note also that gaseous channels were formed along the Ni network as clearly shown in Fig. 3.

Changes in configuration.—The linear shrinkage and the porosity before the reduction were obtained for the new anode and a "YSZ composite," which consists of coarse and fine YSZs alone; those YSZ powders were produced in a similar way of the new anode powders. In Fig. 4, the linear shrinkage of the new anodes and the YSZ composites after sintering in air is plotted against the percentage of coarse YSZ content with respect to the total YSZ content.

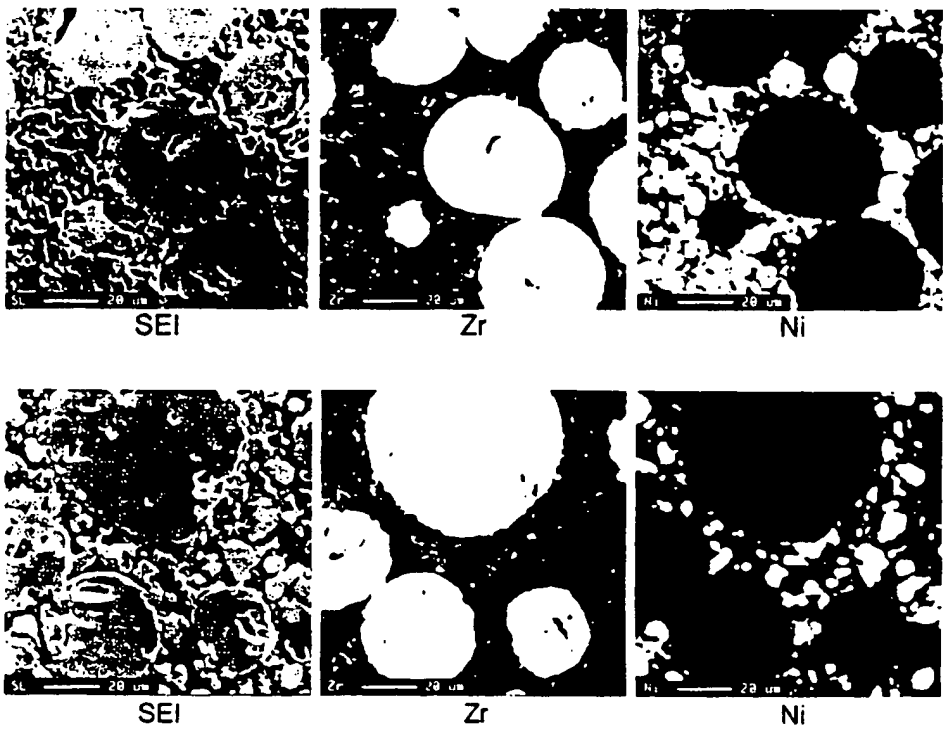

Fig. 3. Typical microstructures of a new anode observed by EPMA; polished cross sections of sintered body, (a) before reduction and (b) after reduction. SEI is an abbreviation for secondary electron image, Zr corresponds to an elemental distribution of zirconia included in YSZ, Ni being an elemental distribution of NiO before reduction or reduced Ni metal.

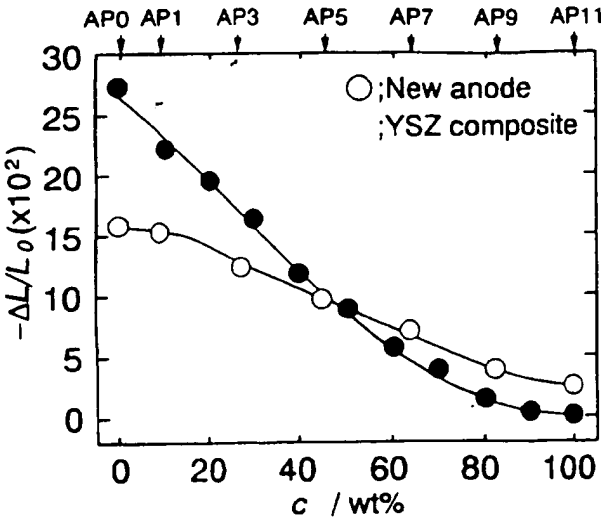

Fig. 4. Linear shrinkage fraction, $-\Delta L/L_0$, of the new anode and the YSZ composite after sintering in air at 1673 K for 10 h as a function of coarse YSZ content, c, of total YSZ. YSZ composites are made of the coarse and fine YSZ in the similar way but without NiO.

It was noted that with increasing coarse YSZ content, the shrinkage of both samples decreased gradually. Figure 5 shows the changes in porosity, showing an opposite trend to that of shrinkage. From Fig. 4 and 5, it can be seen that for the YSZ composite, both shrinkage and porosity slopes are greater than the cermet samples; this indicates that upon the addition of the NiO powder, the cermet densifies less than the composite YSZ when using coarse YSZ powder, but densifies more readily when fine YSZ powder is used.

The shrinkage and the porosity of the reference anode after the same treatment were 15.6 and 14.6%, respectively. The reference anode, when sintered with both a 3 m/o YSZ plate (*ca.* 300 μm) and an 8 m/o YSZ plate (10 cm diam and *ca.* 300 μm) using the same baking process caused warping of the plates due to large shrinkage. Thus, these materials are undesirable, since they will cause shearing stresses at the anode/electrolyte interface during fabrication. The AP11 sample was more crumbly than the samples between AP0 and AP9 after sintering in air. In this sense, the new anodes containing less than 10 w/o of coarse YSZ, namely, AP0 and AP1, and containing no fine YSZ are unsuitable for SOFC anode.

Figure 6 shows the volume shrinkage of samples as a function of holding time in a hydrogen atmosphere. The reference anode contracted at the most significant rate of about 17.0% at 300 h and even after 300 h continued to shrink. This sintering is accompanied with strong agglomeration, leading to the generation of the shearing stress at the interface with electrolyte. When NiO alone was reduced and held for 300 h, porous specimen became agglomerated and shrank more than 50.0%.[16] This difference between the reference anode and NiO alone indicates that the added YSZ powder inhibits the shrinkage of the anode and coarsening of Ni particles. The new anodes containing less than 80 w/o coarse YSZ, namely, AP0 to AP9, showed only a slight volume decrease (less than 3.0%) during the initial 50 h, and then became constant with time. With decreasing coarse YSZ content, the volume contraction becomes more mild and only a small difference is seen between AP0 and AP7.

Figure 7 shows the porosity changes during reduction. The large initial increase in porosity, which occurs for all anode materials, is due to the reduction of NiO to Ni metal. The reference anode then showed a gradual decrease down to about 20%; this was apparently caused by Ni agglomeration. The new anodes did not show any changes after

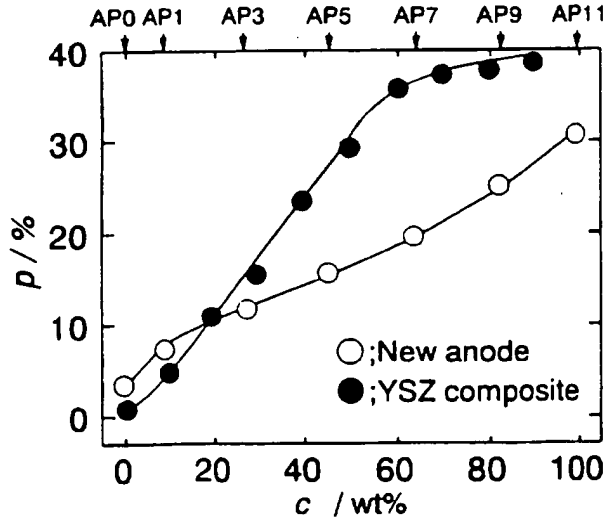

Fig. 5. Changes in porosity, p, of the new anodes and the YSZ composite after sintering in air at 1673 K for 10 h as a function of coarse YSZ content, c, of total YSZ. The value for the reference material was 14.6%.

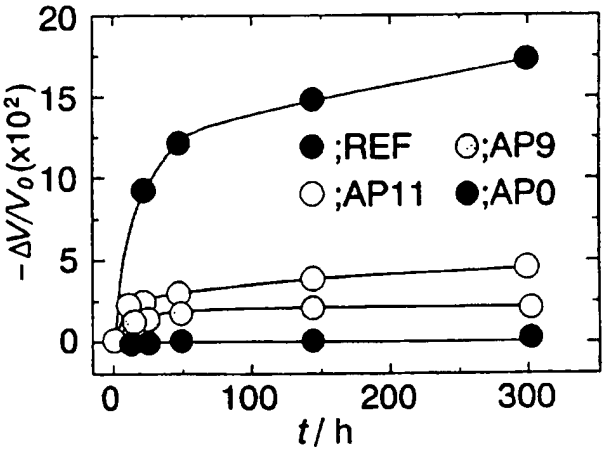

Fig. 6. Changes in volume fraction, $-\Delta V/V_0$, as a function of holding time, t, in a hydrogen atmosphere at 1273 K. The curves on samples from AP1 to AP7 were omitted because they showed similar magnitude and time dependence to AP0. The reference material is coded as "REF."

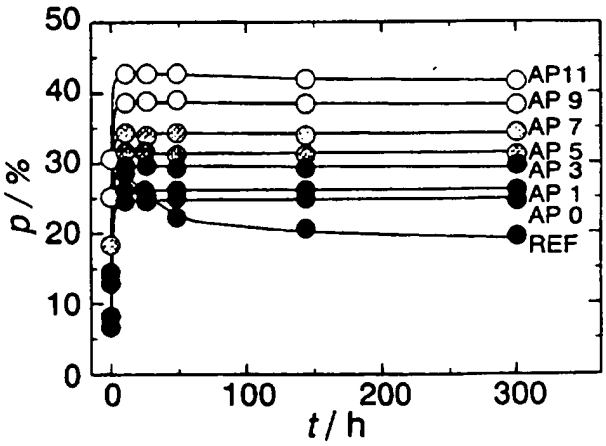

Fig. 7. Changes in porosity, p, as a function of reduction time, t, at 1273 K. The reference material is coded as "REF."

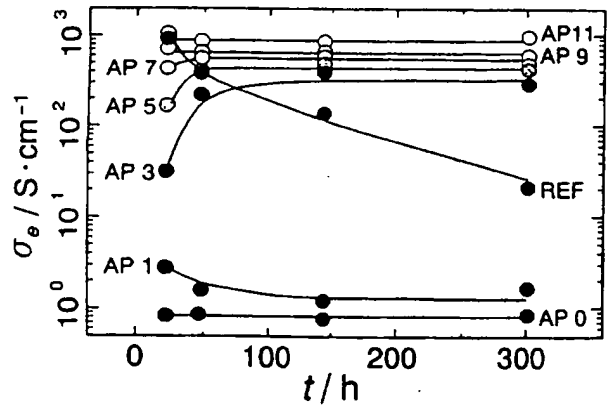

Fig. 8. Electrical conductivity, σ_e, of the new anode and the reference one as a function of reduction time, t, between 24 and 300 h. The reference material is coded as "REF."

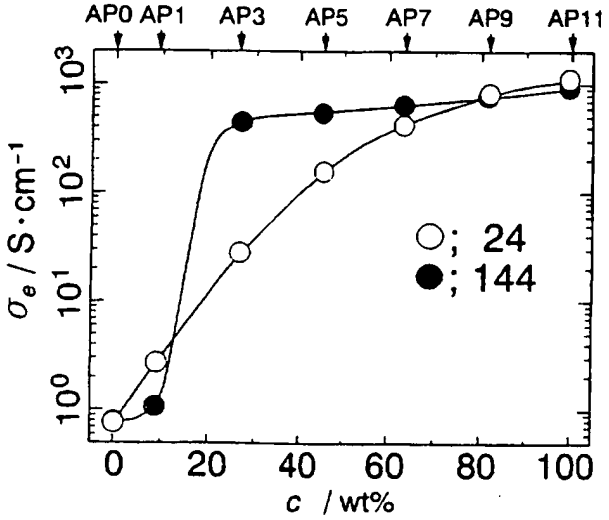

Fig. 9. Electrical conductivity, σ_e, of new anodes in a hydrogen atmosphere at 1273 K as a function of coarse YSZ content, c, of total YSZ. Given numbers of "24" and "144" mean the holding hours.

reduction except a small change at most about 1.0% for AP11, which contained no fine YSZ powder.

The present results on the configurational features suggest that the coarse and fine YSZs form a solid framework in the new materials and prevent damages on the reduction of NiO or the Ni agglomeration.

Change in electrical conductivity.—Figure 8 shows the electrical conductivities of the reference and the new samples as a function of reduction time up to 300 h. The reference anode shows a remarkable decrease in the conductivity with time due to the Ni agglomeration. The low conductivity of AP0 shows that Ni particles are isolated by the YSZ matrix and that good Ni contact is lost. The conductivity of AP1 in the initial stage shows that this is slightly improved when compared with AP0. This indicates that Ni connection is stable initially but gradually degrades with time, probably because the sintering of Ni causes disconnection of Ni particles. The other samples containing more coarse YSZ showed even better behavior for time dependence. That is, their conductivities were rapidly improved in the initial stage and approached rather high values. This initial increment in conductivity is smaller for samples containing more coarse YSZ, indicating that the Ni particles form a better conductive network. Dees *et al.*[17] described that more than 1 h was normally required to attain a steady state for their samples, although more than 90% of the change occurred in the first 10 min. Note that it took more than 50 h to attain the steady state in the new anode materials; this is apparently due to the large size of the coarse YSZ particles. It is likely that it takes larger time for fine YSZ, which is arranged around the coarse YSZ, to form a better Ni network. In order to improve, and/or change, the conductivity of the new anodes, therefore, a longer reducing and sintering time is needed for the cermets consisting of fine particles.

Figure 9 shows the electrical conductivities of the new anodes kept under reducing atmospheres at 24 and 144 h as a function of the coarse YSZ content. Note that the conductivity is improved by three orders of magnitude by increasing the content of the coarse YSZ. The conductivity at 24 h sample increases smoothly with the coarse YSZ content up to 60 w/o, while that at 144 h exhibits an abrupt increase in conductivity at more than 20 w/o. This difference in the conductivity curves can be attributed to the fact that on Ni agglomeration, Ni contact becomes either better or worse depending on the YSZ particle size. Such size effects have been observed in other cermet anodes. For example, Dees *et al.*[17] chose a Ni content of around/over 30 v/o and observed that the particle size is an important factor. Malliaris *et al.*[19] and Aharoni[20] have also investigated the effect of particle size on conductivity of composites made with conductive and insulative powders. They pointed out that the conductivity is directly dependent on the respective volume fractions and also on the respective particle sizes.

Relation between the microstructure and the configurational and the electrical properties.—The configurational and electrical behavior of the reference anode changed most significantly. EPMA observations for this material showed that tiny "detached YSZ particles" were distributed in a highly dispersed manner over the NiO matrix before reduction, and that Ni particles agglomerated at some places after the test. In this case, YSZ was precalcined so that it is quite hard for the particles to cohere with each other; in this sense, we call it the detached YSZ particle. On the other hand, the volume contracts on and the rapid agglomeration occur simultaneously on reduction of NiO to Ni metal, leading to the pore formation in the cermets.[16] This Ni agglomeration in turn causes the gradual rearrangement of the YSZ particles and, as a result, the continual volume shrinkage as well as the de-

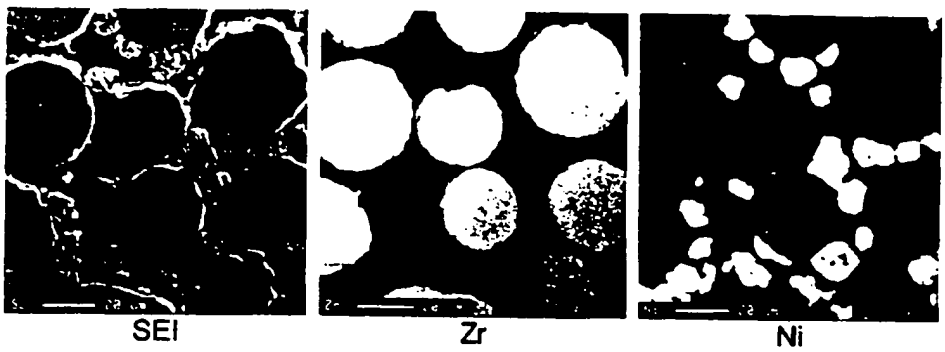

Fig. 10. SEI and elemental distributions of Zr (YSZ) and Ni (Ni metal) on AP11 after 48 h reduction. AP11 without the fine YSZ particles composed of NiO, reduced to metal Ni, and coarse YSZ particles.

crease in porosity. This YSZ was unable to sinter completely and, therefore, formed a loose framework. Although this framework allows the development of a current path, loosely joined YSZ also permits Ni agglomeration and, as a result, disconnection of the current path.

A similar idea can be applied to the configurational behavior of AP11: the only difference between the reference and AP11 anodes is the size of precalcined YSZ particle. In the case of AP11, where the fine YSZ is absent, coarse YSZ particles provide large interstices where almost all NiO particles exist. Micropores and Ni particles can be therefore formed in the interparticle area as shown in Fig. 10. As shown Fig. 6, the configurational change rate was quite small for AP11, compared with the reference anode. The consequent feature observed in the present investigation is that the nonprecalcined fine YSZ plays the most important role of adhering the coarse YSZ particles and stabilizing the YSZ framework as shown in Fig. 6 and 7.

A typical example of effects of microstructure on the conductivity can be obtained by comparing AP0 and AP11. Figure 11 shows the microstructure of AP0 after 48 h reduction; the Ni particles are wrapped by the YSZ matrix produced by the fine YSZ, while AP11 has continuous Ni connection as shown in Fig. 10. The fine YSZ alone built a dimensionally quite stable framework and, as a result, isolated Ni particles without making the Ni connection. Figure 12 shows the microstructure of AP1. This cermet contains the smallest amount of coarse YSZ, where Ni particles are still surrounded by the fine YSZ matrix in a similar manner to AP0. The microstructures of AP3 and AP5, shown in Fig. 13 and 14, indicate that instead of forming the YSZ matrix, YSZ bridges were formed between coarse particles. This allows the Ni particles to form the current paths. As already described above, this Ni path is strengthened by the sintering of Ni. This configurational stability of the new anode should be compared with the reference anode. Its conductivity was initially as high as that of AP11 and decreased gradually with time. This phenomenon can therefore be explained from a configurational point of view; that is, sintering of Ni does not strengthen the Ni network but cut them.

Conclusions

The present investigation has clarified that the microstructure of Ni-YSZ cermet anodes for solid oxide fuel cells has a strong effect on the configurational and electrical behaviors. The reference material, prepared by powder mixture and precalcination process, showed the significant changes under fabrication and operation conditions due to the loose YSZ framework, the decrease in NiO volume, and the rapid Ni agglomeration.

In the novel conceptual anodes described in this paper, coarse YSZ particles are essential for the formation of a

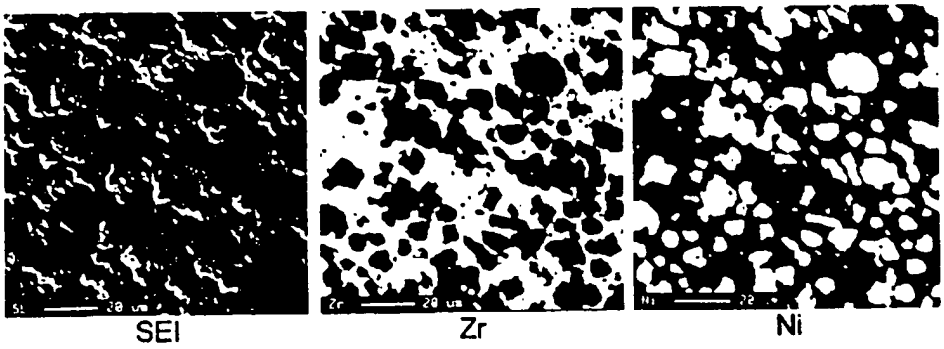

Fig. 11. SEI and elemental distributions of Zr (YSZ) and Ni (Ni metal) of AP0 after 48 h reduction. The polished cross section of sample was observed EPMA. AP0 without the coarse YSZ particles composed of NiO, reduced to metal Ni, and fine YSZ.

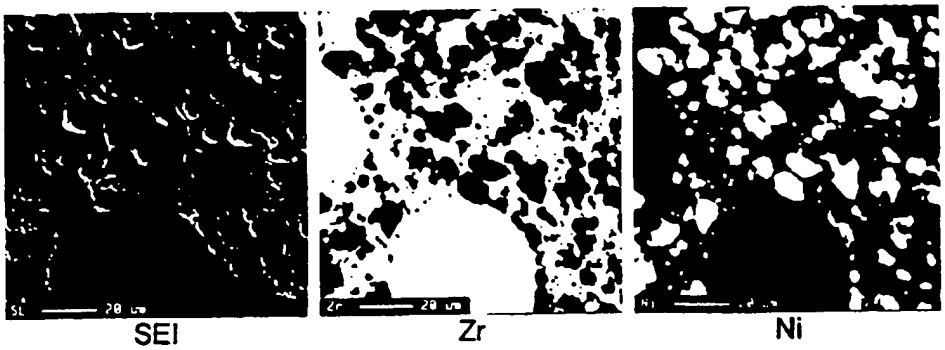

Fig. 12. SEI and elemental distributions of Zr (YSZ) and Ni (Ni metal) on AP1 after 48 h reduction.

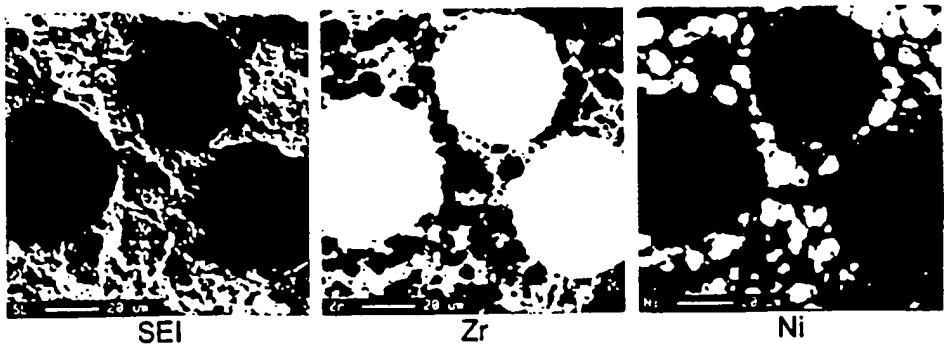

Fig. 13. SEI and elemental distributions of Zr (YSZ) and Ni (Ni metal) on AP3 after 48 h reduction.

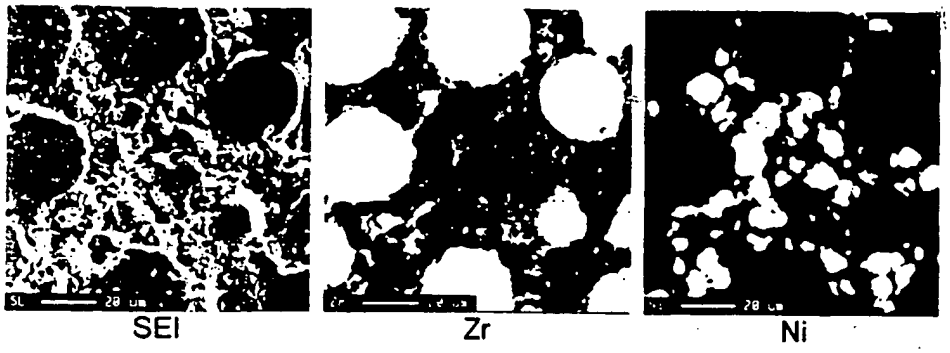

Fig. 14. SEI and elemental distributions of Zr (YSZ) and Ni (Ni metal) on AP5 after 48 h reduction.

YSZ frame which keeps the volume unchanged. Even so, the coarse YSZ particles alone are not appropriate to achieve long-term stability, since slight changes in the volume and the porosity were still observed. The addition of the fine YSZ particles is effective in achieving more stable anode without any substantial decrease in the electrical conductivity and alternation of the microstructural configuration. It is confirmed that the conductivity depends not only on the Ni content but also on the particle size of YSZ and the mixture ratio between the coarse YSZ and the fine YSZ.

Manuscript submitted May 28, 1996; revised manuscript received Nov. 4, 1996.

The Yokosuka Research Laboratory assisted in meeting the publication costs of this article.

REFERENCES

1. N. Q. Minh, *J. Am. Ceram. Soc.*, **76**, 563 (1993).
2. T. Norby, O. J. Velle, H. Leth-Olsen, and R. Tunold, in *Solid Oxide Fuel Cells/1993*, S. C. Singhal and H. Iwahara, Editors, PV 93-4, p. 473, The Electrochemical Society Proceedings Series, Pennington, NJ (1993).
3. G. Maggio, I. Ielo, V. Antonucci, and N. Girodano, in *Solid Oxide Fuel Cells/1991*, F. Grosz, S. C. Singhal, and O. Yamamoto, Editors, EUR 13564, p. 611, Commission of the European Communities Energy, Luxemburg-Belgium (1991).
4. T. Kawada, N. Sakai, H. Yokokawa, M. Dokiya, M. Mori, and T. Iwata, *Solid State Ionics*, **40/41**, 402 (1990).
5. M. Mogensen, S. Primdahl, J. T. Reinländer, S. Gormsen, S. Linderoth, and M. Brown, in *Solid Oxide Fuel Cells/IV*, M. Dokiya, O. Yamamoto, H. Tagawa, and S. C. Singhal, Editors, PV 95-1, p. 657, The Electrochemical Society Proceedings Series, Pennington, NJ (1995).
6. T. Kawada, N. Sakai, H. Yokokawa, M. Dokiya, M. Mori, and T. Iwata, *This Journal*, **137**, 3042 (1990).
7. J. Mizusaki, H. Tagawa, K. Isobe, M. Tajika, I. Koshiro, H. Maruyama, and K. Hirao, *ibid.*, **141**, 1674 (1994).
8. J. Mizusaki, H. Tagawa, T. Saito, T. Yamamura, K. Kamitani, K. Hirao, S. Ehara, T. Takagi, T. Hikita, M. Ippommatsu, S. Nakagawa, and K. Hashimoto, *Solid State Ionics*, **70/71**, 52 (1994).
9. M. Ippommatsu, H. Sasaki, A. Hirao, S. Otoshi, M. Suzuki, and A. Kajiyama, in *IFCC*, p. 349, Makuhari, Japan (1992).
10. M. Suzuki, H. Sasaki, S. Otoshi, A. Kajiyama, and M. Ippommatsu, *Solid State Ionics*, **62**, 125 (1993).
11. S. Murakami, Y. Miyake, Y. Akiyama, N. Ishida, T. Saito, and N. Fukukawa, in *Solid Oxide Fuel Cells-1989, Nagoya*, O. Yamamoto, M. Dokiya, and H. Tagawa, Editors, p. 187, Science House Co., Ltd., Tokyo (1989).
12. C. Iwasawa, M. Nagata, S. Yamaoka, Y. Seino, and M. Ono, in *Solid Oxide Fuel Cells/IV*, M. Dokiya, O. Yamamoto, H. Tagawa, and S. C. Singhal, Editors, PV 95-1, p. 686, The Electrochemical Society Proceedings Series, Pennington, NJ (1995).
13. Y. Takeda, Y. Sakaki, T. Ichikawa, N. Imanishi, O. Yamamoto, M. Mori, N. Mori, and T. Abe, *Solid State Ionics*, **72**, 257 (1994).
14. M. Mori and C. Asakawa, CRIEPI Rep. WE90004 (1990).
15. H. Itoh, T. Yamamoto, M. Mori, and T. Abe, in *Solid Oxide Fuel Cells/IV*, M. Dokiya, O. Yamamoto, H. Tagawa, and S. C. Singhal, Editors, PV 95-1, p. 639, The Electrochemical Society Proceedings Series, Pennington, NJ (1995).
16. H. Itoh, T. Yamamoto, M. Mori, T. Watanabe, and T. Abe, *Denki Kagaku*, **64**, 549 (1996).
17. D. W. Dees, T. D. Claar, T. E. Elser, and F. C. Marzek, *This Journal*, **134**, 2141 (1987).
18. J. R. MacDonald, *Impedance Spectroscopy*, p. 213, John Wiley & Sons, Inc., New York (1987).
19. A. Malliaris and D. T. Turner, *J. Appl. Phys.*, **42**, 614 (1971).
20. S. M. Aharoni, *ibid.*, **43**, 2463 (1972).